Data Collection Maximization for UAV-Enabled Wireless Sensor Networks

Mengyu Chen
The Australian National University
Canberra, ACT 2601, Australia
mengyu.chen1@anu.edu.au

Weifa Liang
The Australian National University
Canberra, ACT 2601, Australia
wliang@cs.anu.edu.au

Yuchen Li
The Australian National University
Canberra, ACT 2601, Australia
yuchen.li@anu.edu.au

***Abstract*—Data collection in wireless sensor networks (WSNs) as a fundamental problem has been extensively studied in the past. With the fast deployment of 5G networks, the use of unmanned aerial vehicles (UAVs) for data collection in WSNs has become a promising technology due to its high flexibility, low cost and ease of deployment. Most existing studies of using UAVs for data collection focused on the one-to-one data collection scheme, where a UAV can collect the sensing data from one sensor at each time. There is another one-to-many data collection scheme where the UAV can collect sensing data from multiple sensors simultaneously through the Orthogonal Frequency Division Multiple Access technique. In this paper, we study data collection in WSNs by adopting the one-to-many data collection scheme with the aim to maximize the volume of data collected, subject to the energy capacity on the UAV. Specifically, we first formulate a novel multi-sensor data collection optimization problem and show that the problem is NP-hard. We then devise a $(1 - \frac{1}{e})$-approximation algorithm for the problem. We finally evaluate the performance of the proposed algorithm through experimental simulations. Simulation results demonstrate that the proposed algorithm is promising, and outperforms other heuristics significantly.**

I. Introduction

Wireless Sensor Networks (WSNs) play important roles in data acquisition, including industrial monitoring [4], healthcare [10], underwater monitoring [16] and smart homes [5]. Each sensor in WSNs is a tiny device with limited energy battery and storage. With the fast deployment of 5G networks, the data generated from various sensor devices will grow exponentially, which will help governments, businesses and organizations for smart management and business decision-making. However, collecting fresh sensing data in WSNs becomes crucial to avoid data loss and data overwritten. The unmanned aerial vehicle (UAV) has emerged as a promising technology for data collection in WSNs, due to its autonomy and flexibility [3]. However, the UAV is required to be replenished quite often, due to its limited energy capacity, which poses many challenges. For example, the energy supply of a UAV may not be able to collect data from all sensors in a monitoring region, then which sensors' data should the UAV collect? To maximize the volume of the collected data, at which locations should the UAV hover and how long should it stay at each hovering location? In this paper we will address these challenges.

Extensive studies of data collection in WSNs have been conducted in the past. For example, Zhan *et al.* [17] jointly considered working states of sensors and the trajectory of the UAV by utilizing a fading channel model for the senor-UAV links to minimize the maximum energy consumption of sensors. Binol *et al.* [1] aimed at finding a time-optimal path for each of multiple UAVs for data collection from roadside units. These studies of data collection are based on the one-to-one data collection scheme, in which a UAV can collect sensing data from one sensor only at each time. On the other hand, there are several other studies under the one-to-many data collection scheme where a UAV can collect sensing data from multiple sensors simultaneously as long as the UAV is within the transmission ranges of the sensors. For example, Mozaffari *et al.* [11] assumed that IoT devices can transmit their data by adopting the Orthogonal Frequency Division Multiple Access (OFDMA) technique, such that a UAV can support multiple IoT devices simultaneously. They dealt with the finding of an optimal trajectory for each of multiple UAVs to minimize the transmission energy consumption of ground IoT devices. Ghorbel *et al.* [2] focused on the identification of optimal locations for a single UAV to collect data from a cluster of sensors with the aim of minimizing the energy consumption of the UAV. Samir *et al.* [14] considered a scenario where a UAV is dispatched for data collection from time-constrained devices and each device had a data uploading deadline, aiming at maximizing the network throughput. Li *et al.* [7] considered data collection in WSNs by taking into account both hovering energy and traveling energy consumptions of an energy-constrained UAV, and developed efficient approximation and heuristic algorithms for the problem. Unlike most aforementioned studies that the data from all sensors within the data reception range of the UAV must be fully collected, in this paper we assume that the data stored at a sensor can be partially collected and can be collected through multiple times by the UAV per tour. We study data collection in WSNs via an energy-constrained UAV [9] under one-to-many data collection scheme with the aim to maximize the volume of collected data.

The novelties of this study lie in that a novel data collection problem via the use of UAV is formulated and a performance-guaranteed approximation algorithm for the problem is devised.

The main contributions of the paper are as follows.

- We formulate a novel Multi-sensor data collection Opti-

978-1-7281-6607-0/20/$31.00 ©2020 IEEE

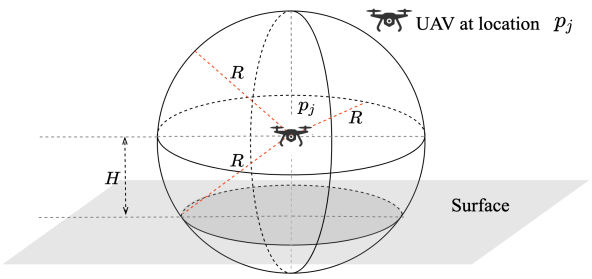

Fig. 1: The sphere O_j with center p_j and radius R.

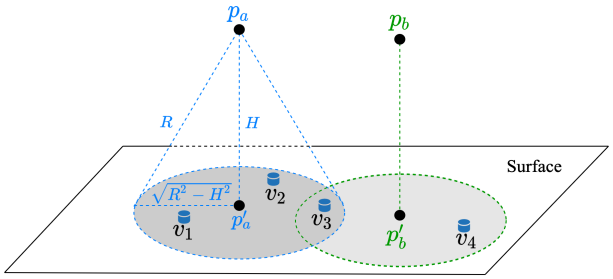

Fig. 2: p'_a and p'_b are projections of p_a and p_b on the ground. We have that $S_a = \{v_1,\ v_2,\ v_3\}$, $S_b = \{v_3,\ v_4\}$, $L_1 = \{p_a\}$, $L_2 = \{p_a\}$, $L_3 = \{p_a,\ p_b\}$, $L_4 = \{p_b\}$.

mization Problem (MOP) to maximize the volume of data collected under the assumption that the UAV can collect data from multiple sensors simultaneously, and show that the problem is NP-hard.

- We devise an approximation algorithm with a $(1 - \frac{1}{e})$ approximation ratio for the problem.
- We evaluate the performance of the proposed algorithm through extensive experimental simulations. Simulation results demonstrate that the proposed algorithm is promising.

The remainder of the paper is organized as follows. Section II introduces the UAV data collection model for WSNs and defines the problems. The NP-hardness of the defined problems is also shown in this section. Section IV deals with a special case of the MOP and an optimal algorithm for this special case is proposed. Section V studies the MOP, and an approximation algorithm for it is devised. Section VI evaluates the performance of the proposed algorithms, and Section VII concludes the paper.

II. Preliminaries

In this section, we first introduce the system and data collection models. We then define the problem precisely. We finally show the NP-hardness of the defined problem.

A. System Model

We consider a WSN, where $\mathcal{V} = \{v_i \mid 1 \leq i \leq N\}$ is a set of homogeneous sensor nodes deployed over a two-dimensional region on the ground. Let $(x_i, y_i, 0)$ denote the location of sensor v_i. We assume that each sensor node v_i has a fixed data transmission range R and an identical data transmission bandwidth B, with a volume D_i of data stored locally to be collected. A UAV is deployed for sensory data collection in the WSN, with a fixed hovering altitude H. Considering the energy capacity constraint of the UAV, we assume that the maximum number of hovering (equal) time slots of the UAV per tour is Γ. Supported by OFDMA technique [11], the UAV is able to collect data from multiple sensors simultaneously.

B. The Data Collection Model

We assume that a set $\mathcal{P} = \{p_j = (X_j, Y_j, H) \mid 1 \leq j \leq M\}$ of potential hovering locations is given, where the UAV can only hover at locations in $\mathcal{P}$ for data collection. Under the one-to-many data collection scheme, where each sensor has an identical data transmission range R, it is equivalent to regard the UAV to be with a data reception range R. As shown in Fig. 1, for each given location $p_j = (X_j, Y_j, H)$, a sphere O_j with center p_j and radius R can be obtained. When the UAV hovers at p_j, a location (x, y, z) is within the data reception range of the UAV, if and only if it locates within the space of O_j (including the surface of O_j), i.e.,

$$(x - X_j)^2 + (y - Y_j)^2 + (z - H)^2 \leq R^2. \tag{1}$$

Denote by p'_j the projection of p_j on the ground, i.e., $p'_j = (X_j, Y_j, 0)$. If a location $(x, y, 0)$ on the ground is within the data reception range of the UAV, it is equivalent to say, the Euclidean distance between the location and p'_j is no greater than $\sqrt{R^2 - H^2}$. For a given location $p_j \in P$, its *data collection sensor set* S_j is a subset of sensors in $\mathcal{V}$, whose Euclidean distance from p'_j is no greater than $\sqrt{R^2 - H^2}$, i.e.,

$$S_j = \{v_i \mid (x_i - X_j)^2 + (y_i - Y_j)^2 \leq R^2 - H^2,\ v_i \in \mathcal{V}\}. \tag{2}$$

For a given sensor $v_i \in V$, its *data collection location set* L_i is a subset of locations in $\mathcal{P}$, in which each location p_j is within the data transmission range of sensor $v_i \in \mathcal{V}$, i.e.,

$$L_i = \{p_j \mid (x_i - X_j)^2 + (y_i - Y_j)^2 \leq R^2 - H^2, \\ p_j \in \mathcal{P}\}. \tag{3}$$

Under the one-to-many data collection scheme, the UAV can collect sensory data from all sensors in S_j simultaneously when it hovers at location p_j. In other words, the data of sensor v_i can be collected by the UAV when the UAV hovers at any location in L_i. We thus have $v_i \in S_j$ if and only if $p_j \in L_i$. Fig. 2 is an example to illustrate the relationships between the data collection sensor set S_j and the data collection location set L_i.

Although the one-to-many data collection scheme can significantly improve data collection efficiency, an energy-constrained UAV usually cannot collect all sensory data from a large-scale WSN, due to its energy capacity constraint. In this paper, we refer to the energy capacity constraint on the UAV as the maximum hovering duration of the UAV per tour, and we further divide the hovering duration of the UAV per tour into Γ equal *time slots* with each having length τ [9]. Denote

by $\mathcal{T} = \{T_j \mid T_j \geq 0,\ p_j \in \mathcal{P}\}$ a set of hovering durations (in terms of time slots) of the UAV at different locations $p_j \in \mathcal{P}$. The total hovering duration of the UAV per tour thus is no greater than Γ time slots, i.e.,

$$\sum_{T_j \in \mathcal{T}} T_j \leq \Gamma. \tag{4}$$

Denote by C_i the total amount of data collected from sensor v_i by the UAV at hovering locations in L_i, which can be calculated as follows.

$$C_i = \sum_{p_j \in L_i} B \cdot \tau \cdot T_j. \tag{5}$$

As each sensor v_i has a data volume D_i initially, the total volume of data collected by the UAV per tour thus is

$$\sum_{v_i \in \mathcal{V}} \min\{C_i,\ D_i\}. \tag{6}$$

C. Problem Definitions

In the following we define two novel data collection optimization problems under the one-to-many data collection scheme.

The *Multi-sensor data collection Optimization Problem (MOP)*: Given a WSN with a set $\mathcal{V} = \{v_i \mid 1 \leq i \leq N\}$ of sensors on the ground, a UAV with the maximum number of hovering time slots Γ per tour is deployed for data collection in the WSN under the one-to-many data collection scheme. Each sensor $v_i \in \mathcal{V}$ has a volume D_i of data to be collected, assuming that each sensor has a data transmission range R with transmission bandwidth B. A set $\mathcal{P} = \{p_j = (X_j, Y_j, H) \mid 1 \leq j \leq M\}$ of potential hovering locations with altitude H for the UAV is given, where the UAV can only hover at the locations in $\mathcal{P}$ for data collection. The problem is to identify which locations in $\mathcal{P}$ will be the hovering locations of the UAV, and to determine the hovering duration at each identified hovering location under the energy constraint of the UAV, such that the total volume of data collected from sensors is maximized, subject to Γ time slots per tour, i.e.,

$$maximize \quad \sum_{v_i \in \mathcal{V}} min\{C_i,\ D_i\}. \tag{7}$$

$$s.t. \quad \sum_{T_j \in \mathcal{T}} T_j \leq \Gamma, \tag{8}$$

$$0 \leq T_j \leq \Gamma, \tag{9}$$

$$Eq.\ (3),\ (5). \tag{10}$$

We now define the *Multi-sensor data collection Optimization with hovering location Constraint Problem (MOCP)*, which is a special case of the defined MOP, where the Euclidean distance $DIS(p_a,\ p_b)$ between any two hovering locations p_a and p_b in $\mathcal{P}$ is strictly larger than $2\sqrt{R^2 - H^2}$, i.e., $DIS(p_a,\ p_b) > 2\sqrt{R^2 - H^2}$.

To tackle the MOP, in this paper we first study one of its variants – the *Maximum Coverage with Height problem (MCH)* defined as follows.

Given a vertex set $\mathcal{V} = \{v_i \mid 1 \leq i \leq N\}$ and an integer $K \geq 1$, let $\mathcal{S} = \{S_j \mid 1 \leq j \leq M\}$ be a collection of subsets on $\mathcal{V}$. Associated with each vertex $v_i \in \mathcal{V}$, there is a height h_i with the initial value $h_i^0 \geq 0$, and the value of h_i is updated to $\max\{h_i - 1,\ 0\}$ if a set S_j containing v_i is chosen. To be specific, denote by h_i' and h_i'' the heights of v_i before and after selecting S_j respectively. Then, the decrement of the height of v_i caused by the selection of S_j is

$$h_i' - h_i'' = \begin{cases} 1, & \text{if } v_i \in S_j \text{ and } h_i' \geq 1 \\ h_i', & \text{if } v_i \in S_j \text{ and } h_i' < 1 \\ 0, & \text{otherwise.} \end{cases} \tag{11}$$

The MCH is to select K subsets from $\mathcal{S}$ such that the total height decrement of vertices in $\mathcal{V}$ is maximized.

III. NP Hardness of Problems

In the following we show that both MCH and MOP are NP-hard.

Theorem 1: The Maximum Coverage with Height problem (MCH) is NP-hard.

Proof We prove the NP-hardness of the MCH through a reduction from a well-known NP-hard problem - the *maximum coverage problem* (MCP). An instance of the MCP can be reduced to an instance of the MCH, where each vertex $v_i \in \mathcal{V}$ in MCP has an initial height $h_i^0 = 1$. It can be seen that a solution to the MCH returns a solution to the MCP, and the reduction is polynomial. The theorem thus follows. □

Theorem 2: The Multi-sensor data collection Optimization Problem (MOP) is NP-hard.

Proof We show the NP-hardness of the MOP through a reduction from the MCH. For each instance M_1 of the MCH, it can be reduced to an instance M_2 of the MOP as follows. Let $\Gamma = K$, then the number K of selected sets of M_1 correspond the number $\Gamma = K$ of hovering time slots of UAV in M_2. The set $\mathcal{V}_1$ in M_1 corresponds to a set $\mathcal{V}_2$ of sensors in M_2, while each set S_j in M_1 corresponds to a potential hovering location p_j' with the data collection sensor set S_j', such that for each vertex $v_i \in S_j$ with height h_i, there exists a corresponding sensor $v_i' \in S_j'$, with $D_i' = h_i \cdot B \cdot \tau$ volume of data to be collected, where B is the data transmission bandwidth and τ is the length of each time slot. The MOP is to maximize the volume of collected data by selecting the hovering locations in $\mathcal{P}$ with durations for the UAV, subject to Γ $(= K)$ hovering time slots. It can be seen that a solution to M_2 returns a solution to M_1, and the reduction is polynomial. The theorem thus follows. □

IV. An Optimal Algorithm for the MOCP

In this section, we consider the special case MOCP of the MOP, where the Euclidean distance between any two locations in $\mathcal{P}$ is strictly larger than $2\sqrt{R^2 - H^2}$, for which we propose an optimal algorithm as follows.

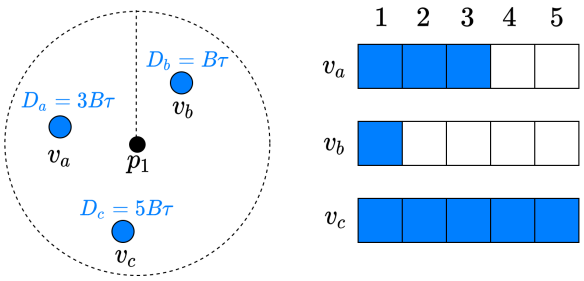

Fig. 3: An illustration of data collected by the UAV at location p_1, where $S_1 = \{v_a,\ v_b,\ v_c\}$ and the data volume stored at each sensor is $D_a = 3B\tau$, $D_b = B\tau$ and $D_c = 5B\tau$ respectively.

A. Profit Function

Following the definition of the MOCP, the Euclidean distance $DIS(p_a, p_b)$ between any two locations $p_a,\ p_b \in \mathcal{P}$ is

$$DIS(p_a, p_b) > 2\sqrt{R^2 - H^2}, \tag{12}$$

where $\mathcal{P} = \{p_j \mid 1 \le j \le M\}$ is the set of potential hovering locations. Under this assumption, there is no overlapping between S_a and S_b when the UAV hovers at locations p_a and p_b with $p_a \neq p_b$, respectively, i.e.,

$$S_a \cap S_b = \emptyset, \quad \forall p_a,\ p_b \in \mathcal{P}. \tag{13}$$

Without loss of generality, we assume that $\cup_{j=1}^{M} S_j = \mathcal{V}$. Then, for each sensor $v_i \in \mathcal{V}$, there is exactly one hovering location $p_j \in \mathcal{P}$ within the data transmission range of v_i, i.e.,

$$|L_i| = 1, \quad \forall v_i \in \mathcal{V}, \tag{14}$$

$$L_i = \{p_j\}, \quad \text{if } v_i \in S_j. \tag{15}$$

A *p_j-located time slot* is referred as a time slot when the UAV hovers at p_j. Recall that T_j is the number of time slots when the UAV hovers at location p_j, which indicates that the hovering duration of the UAV at p_j consists of T_j p_j-located time slots. In the following, we focus on the volume of data collected with the tth p_j-located time slot, where $1 \le t \le T_j$.

Denote by $u_j(t)$ the *profit function* as the volume of data collected at the tth p_j-located time slot. In the following, we show an example of $u_j(t)$ in Fig. 3, where $S_1 = \{v_a,\ v_b,\ v_c\}$ and the data volume stored at each sensor is $D_a = 3B\tau$, $D_b = B\tau$ and $D_c = 5B\tau$ respectively. It can be seen that, at the first $(t = 1)$ p_1-located time slot, the UAV can collect data from sensors v_a, v_b and v_c, with the data volume $u_1(1) = 3B\tau$ of collected data; at the second $(t = 2)$ and third $(t = 3)$ p_1-located time slots, data from sensors v_a and v_c are collected with $u_1(2) = 2B\tau$ and $u_1(3) = 2B\tau$, while for the p_1-located time slots with $t = 4$ and $t = 5$, we have that $u_1(4) = B\tau$ and $u_1(5) = B\tau$.

Denote by l_i the maximum number of time slots when the UAV can collect all data from v_i, i.e.,

$$l_i = \frac{D_i}{B\tau}. \tag{16}$$

Note that, since τ can be set properly, for the sake of convenience, we assume that l_i is an integer.

Denote by $f_i(t)$ a binary variable indicating whether sensor v_i still has remaining data to be collected at the tth p_j-located time slot when the UAV hovers at location p_j in L_i:

$$f_i(t) = \begin{cases} 1, & 0 \le t \le l_i, \\ 0, & \text{otherwise.} \end{cases} \tag{17}$$

The profit function $u_j(t)$ of the UAV at the tth p_j-located time slot is

$$u_j(t) = B \cdot \tau \sum_{v_i \in S_j} f_i(t). \tag{18}$$

An example of the profit function $u_j(t)$ is shown in Fig. 4.

Let $l_{max} = \max\{l_i \mid v_i \in S_j\}$. We define *a drop point* d_k as a time slot where $u_j(d_k) > u_j(d_k+1)$ with $0 < d_k \le l_{max}$, where k indicates that d_k is the kth drop point of the value of $u_j(t)$. Denote by $d_{K_{max}}$ the drop point with $u_j(d_{K_{max}}+1) = 0$, where $d_{K_{max}} = l_{max}$.

Theorem 3: The defined profit function $u_j(t)$ has the following properties for all t with $1 \le t \le l_{max}$.

1) $u_j(t)$ is non-increasing. For any $0 < a < b \le l_{max}$, where $a,\ b \in \mathbb{N}^+$, $u_j(a) \ge u_j(b) > 0$.
2) $u_j(t)$ is a piecewise constant function. The value of $u_j(t)$ is in a finite set $\{u_j(d_k) \mid 1 \le k \le K_{max}\}$ with $u_j(d_k + \Delta) = u_j(d_{k+1})$, where $1 \le \Delta \le d_{k+1} - d_k,\ k+1 \le K_{max},\ \Delta \in \mathbb{N}^+$.
3) The decrement at a drop point is determined by the number of sensors in S_j which finish their data transmission at the drop point, i.e., $u_j(d_k) - u_j(d_k+1) = \sum_{v_i \in S_j}(f_i(d_k) - f_i(d_k+1)) \cdot B \cdot \tau$, with $1 \le k \le K_{max},\ k \in \mathbb{N}^+$, where $\sum_{v_i \in S_j}(f_i(d_k) - f_i(d_k+1))$ is the number of sensors in S_j that finish their data transmission at the d_kth p_j-located time slot.
4) The number of time slots between two consecutive drop points in $u_j(t)$ is determined by the minimum remaining data of sensors in S_j at the previous drop point. For two consecutive drop points d_k and d_{k+1}, denote by D_k^{min} the minimum remaining data among sensors in S_j at d_k, then $d_{k+1} - d_k = \frac{D_k^{min}}{B\tau}$, where $1 \le k \le K_{max} - 1,\ k \in \mathbb{N}^+$.

B. Optimal Algorithm

We propose a time-slot-based algorithm for the MOP by utilizing the defined profit function. The detailed algorithm is shown in `Algorithm 1`. We first calculate the profit function of each potential charging location in $\mathcal{P}$. As mentioned before, l_{max} indicates the maximum number of time slots when the UAV can collect data at location p_j, where $u_j(l_{max}) > 0$ and $u_j(l_{max}+1) = 0$. Note that once the value of a profit function at a hovering location is determined, the value would not change later (Step 2 to Step 5 in the proposed algorithm). The hovering duration at each location in $\mathcal{P}$ is initialized as 0. The algorithm then proceeds iteratively, and there are Γ iterations. Within each iteration, a time slot is allocated to a

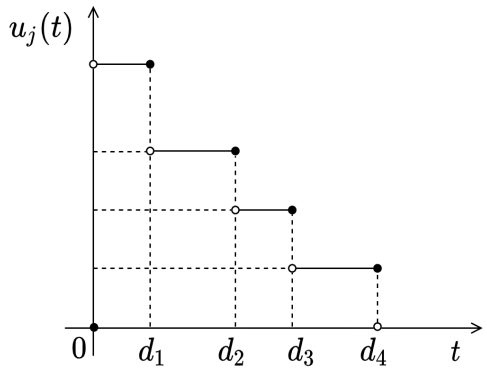

Fig. 4: An instance of the profit function $u_j(t)$.

location in $\mathcal{P}$. T_j is the number of iterations so far when p_j has been selected as a hovering location. Then, at the current iteration, we allocate a time slot to a location that a maximum profit gain can be achieved, i.e., a location $p_{j^{max}} \in \mathcal{P}$ with the maximum value of $u_j(T_j+1)$ is chosen, and a time slot is allocated at location $p_{j^{max}}$, by increasing its hovering duration $T_{j^{max}}$ by 1 (Step 6 to Step 9 of the proposed algorithm). Finally, any location p_j in $\mathcal{P}$ with $T_j > 0$ is identified as one of the hovering locations of the UAV during a data collection tour, and the UAV will hover at location $p_j \in \mathcal{F}$ for $T_j > 0$ time slots, before moving to the next hovering location.

Algorithm 1 Algorithm for the MOCP

Input: A set $\mathcal{V} = \{v_i \mid 1 \le i \le N\}$ of sensors; a set $\mathcal{P}$ of potential hovering locations for the UAV; a family $\mathcal{S} = \{S_j \mid p_j \in \mathcal{P}\}$ of data collection sensor sets for the set $\mathcal{P}$ of locations; the maximum number of hovering time slots Γ for the UAV per tour.

Output: $\mathcal{F} = \{(p_j, T_j) \mid p_j \in \mathcal{P},\ T_j \ge 1\}$: a set of selected hovering locations for the UAV and the corresponding hovering durations;

1: $\mathcal{F} \leftarrow \emptyset$;
2: **for** each $p_j \in \mathcal{P}$ **do**
3: $l_{max} \leftarrow \max\{l_i \mid v_i \in S_j\}$; /* find the maximum value among sensors in S_j */
4: **for** $t \leftarrow 1$ to $l_{max}+1$ **do**
5: $u_j(t) \leftarrow B\tau \cdot \sum_{v_i \in S_j} f_i(t)$;
6: $\mathcal{T} \leftarrow \{T_j \leftarrow 0 \mid p_j \in \mathcal{P}\}$;
7: **for** $I \leftarrow 1$ to Γ **do**
8: Identify a hovering location $p_{j^{max}}$ s.t. $j^{max} \leftarrow \text{argmax}_{p_j \in \mathcal{P}} u_j(T_j+1)$;
9: $T_{j^{max}} \leftarrow T_{j^{max}} + 1$;
10: **for** each $p_j \in \mathcal{P}$ **do**
11: **if** $T_j \ge 1$ **then**
12: $\mathcal{F} \leftarrow \mathcal{F} \cup \{(p_j,\ T_j)\}$;
13: **return** $\mathcal{F}$

C. Algorithm Analysis

The rest is to show that `Algorithm 1` delivers an optimal solution for the MOCP.

Lemma 1: Denote by $\mathcal{T}^* = \{T_j^* \mid 0 \le T_j^* \le \Gamma,\ p_j \in \mathcal{P}\}$ the set of durations for locations in $\mathcal{P}$ delivered by `Algorithm 1`. Then, $u_a(T_a^*) \ge u_b(T_b^*+1)$ for any pair of locations $p_a,\ p_b \in \mathcal{P}$ with $T_a^* \ge 1$.

Proof We prove the claim by contradiction. Assume that there exist T_a^* and T_b^* such that $u_a(T_a^*) < u_b(T_b^*+1)$. Following `Algorithm 1`, assume at iteration t', T_a^* increases from T_a^*-1 to T_a^* when $T_b = T_b' \le T_b^*$, we then have $u_b(T_b') \ge u_b(T_b^*) \ge u_b(T_b^*+1)$, since $u_b(t)$ is a non-increasing function, by Theorem 3. On the other hand, assuming $u_a(T_a^*) < u_b(T_b^*+1)$, we have $u_b(T_b') \ge u_b(T_b^*) \ge u_b(T_b^*+1) > u_a(T_a^*)$. By Step 7 to Step 9 of `Algorithm 1`, T_b should increase from T_b' to $T_b'+1$, instead of that T_a increases from T_a^*-1 to T_a^*. This results in a contradiction. □

Lemma 2: For any hovering duration set $\mathcal{T} = \{T_j \mid 0 \le T_j \le \Gamma,\ p_j \in \mathcal{P}\}$, where $u_a(T_a) \ge u_b(T_b+1)$ for any $T_a,\ T_b \in \mathcal{T}$ with $T_a > 0$ and $\sum_{T_j \in \mathcal{T}} T_j = \Gamma$, it leads to a maximum volume of data collected by the UAV when it hovers at the locations in $\mathcal{P}$ with the hovering durations in $\mathcal{T}$ greater than zeros.

Proof We consider a general case where not all sensory data in a WSN can be fully collected, due to the energy capacity on the UAV. It is to collect as much data as possible by the UAV, the total UAV hovering duration of the optimal solution thus must be exactly Γ time slots. In the following, we prove the claim by contradiction. Assume that there exists a hovering duration set $\mathcal{T}' = \{T_j' \mid p_j \in \mathcal{P}\}$ with $\sum_{T_j \in \mathcal{T}} T_j = \Gamma$, in which there exist $T_a' \ge 1$ and T_b' with

$$u_a(T_a') < u_b(T_b'+1), \tag{19}$$

which results in an optimal solution.

Denote by U' the total volume of data collected by the scheduling $\mathcal{T}'$, i.e.,

$$U' = \sum_{t=0}^{T_a'} u_a(t) + \sum_{t=0}^{T_b'} u_b(t) + \Big(\sum_{p_j \in \mathcal{P}} \sum_{t=0}^{T_j'} u_j(t) - \sum_{t=0}^{T_a'} u_a(t) - \sum_{t=0}^{T_b'} u_b(t)\Big) \tag{20}$$

Let $\mathcal{T}'' = \{T_j'' \mid p_j \in \mathcal{P}\}$ denote a hovering duration set with $T_a'' = T_a' - 1$, $T_b'' = T_b' + 1$ and $T_j'' = T_j'$ for $j \ne a,\ b$. Denote by U'' the total volume of collected data by $\mathcal{T}''$, i.e.,

$$U'' = \sum_{t=0}^{T_a'-1} u_a(t) + \sum_{t=0}^{T_b'+1} u_b(t) + \Big(\sum_{p_j \in \mathcal{P}} \sum_{t=0}^{T_j'} u_j(t) - \sum_{t=0}^{T_a'} u_a(t) - \sum_{t=0}^{T_b'} u_b(t)\Big) \tag{21}$$

Then, we have

$$U'' - U' = \sum_{t=0}^{T'_a-1} u_a(t) + \sum_{t=0}^{T'_b+1} u_b(t) - (\sum_{t=0}^{T'_a} u_a(t) + \sum_{t=0}^{T'_b} u_b(t)) \quad (22)$$

$$= -u_a(T'_a) + u_b(T'_b + 1) \quad (23)$$

$$> 0 \quad \text{(by 19)} \quad (24)$$

It can be seen that the volume of data collected by $\mathcal{T}''$ is larger than the one by $\mathcal{T}'$, which contradicts the assumption that $\mathcal{T}'$ will lead to an optimal solution. The lemma thus follows. □

Theorem 4: `Algorithm 1` for the MOCP delivers an optimal solution.

Proof Denote by $\mathcal{T}^* = \{T_j^* \mid 0 \leq T_j^* \leq \Gamma,\ p_j \in \mathcal{P}\}$ the hovering duration set delivered by `Algorithm 1`. Since there are Γ iterations in `Algorithm 3`, a time slot is allocated to a hovering location in $\mathcal{P}$ at each iteration, and we have $\sum_{T_j^* \in \mathcal{T}^*} = \Gamma$ time slots to be allocated.

By Lemma 1, it has shown that for any two hovering durations $T_a^* \geq 1$ and T_b^* in $\mathcal{T}^*$ delivered by `Algorithm 1`, $u_a(T_a^*) \geq u_b(T_b^* + 1)$. Meanwhile, by Lemma 2, for any hovering duration set $\mathcal{T} = \{T_j \mid p_j \in \mathcal{P}\}$ where $u_a(T_a) \geq u_b(T_b + 1)$ for any $T_a,\ T_b \in \mathcal{T}$ with $T_a \geq 1$ and $\sum_{T_j} = \Gamma$, it will lead to an optimal solution. Thus, the hovering duration at each location in the solution delivered by `Algorithm 1` will result in the maximum volume of data collected, and the solution is optimal. □

V. Approximation Algorithm for the MOP

In this section, we investigate the MOP, by devising an approximation algorithm for it. We start with an approximation algorithm for its variant - the MCH first. We then show how to extend the proposed algorithm to solve the MOP.

A. Approximation Algorithm for the MCH

Recall in the definition of MCH in Section II-C, each vertex v_i in $\mathcal{V}$ has a variable height h_i, which is likely to reduce if a set S_j covering v_i is selected. The MCH is to maximize the total height decrement of vertices in $\mathcal{V}$ by choosing K sets where K is given in advance. The algorithm for the MCH proceeds iteratively. Within iteration k with $1 \leq k \leq K$, a set S^k is selected. Denote by h_i^k the height of v_i after S^k is selected, then

$$h_i^k = \begin{cases} \max\{h_i^{k-1} - 1,\ 0\}, & \text{if } v_i \in S^k, \\ h_i^{k-1}, & \text{otherwise}, \end{cases} \quad (25)$$

where h_i^0 is the initial height of v_i. The MCH thus is to identify a collection of sets $\{S^1, S^2,\ ...,\ S^K\}$ such that $\sum_{v_i \in \mathcal{V}}(h_i^0 - h_i^K)$ is maximized.

In the following we develop an approximation algorithm with a provable $(1 - \frac{1}{e})$ ratio for the MCH.

The core idea behind the proposed algorithm proceeds iteratively. Let $\mathcal{Y}$ be the collection of chosen sets so far. With each iteration k with $1 \leq k \leq K$, a set from the collection $\mathcal{S} \setminus \mathcal{Y}$ is chosen such that the accumulative height decrement of sensors in iteration k is maximized, i.e., a set with index j^{max} will be chosen where

$$j^{max} = \text{argmax}_{S_{j^{max}} \in \mathcal{S} \setminus \mathcal{Y}} \sum_{v_i \in S_{j^{max}}} (h_i^{k-1} - h_i^k). \quad (26)$$

By Eq. (25), Eq. (26) can be rewritten as

$$j^{max} = \text{argmax}_{S_{j^{max}} \in \mathcal{S} \setminus \mathcal{Y}} \sum_{v_i \in S_{j^{max}}} \min\{h_i^{k-1},\ 1\}. \quad (27)$$

The detailed algorithm for the MCH is given in `Algorithm 2`.

Algorithm 2 Algorithm for the MCH

Input: A set $\mathcal{V} = \{v_i \mid 1 \leq i \leq N\}$, where each vertex $v_i \in \mathcal{V}$ has a initial height h_i^0; a collection of vertex sets $\mathcal{S} = \{S_j \mid 1 \leq j \leq M\}$; a fixed K, which is the number of sets to be selected from $\mathcal{S}$.

Output: The K chosen sets.

$\mathcal{U} \leftarrow \mathcal{S}$;
$\mathcal{Y} \leftarrow \emptyset$; /* the solution */
for $k \leftarrow 1$ to K **do**
  $j^{max} \leftarrow \text{argmax}_{S_{j^{max}} \in \mathcal{U}} \sum_{v_i \in S_{j^{max}}} \min\{h_i^{k-1},\ 1\}$;
  $S^k \leftarrow S_j^{max}$;
  $\mathcal{Y} \leftarrow \mathcal{Y} \cup \{S^k\}$; $\mathcal{U} \leftarrow \mathcal{U} \setminus \{S^k\}$;
  for each $v_i \in \mathcal{V}$ **do**
    if $v_i \in S^k$ **then**
      $h_i^k \leftarrow \max\{h_i^{k-1} - 1,\ 0\}$;
    else
      $h_i^k \leftarrow h_i^{k-1}$;
return $\mathcal{Y}$

B. Approximation Algorithm for the MOP

The basic idea of an algorithm for the MOP is similar to the one for the MCH, which also proceeds iteratively. There are Γ iterations (as there are Γ time slots per tour of the UAV). Within iteration k, a set S^k is chosen. The rest is how to modify `Algorithm 2` for the MOP. To this end, the sensor heights and the formation of sets should be given as follows.

Sensor Height Determination: Denote by h_i^k the height of sensor v_i after a set S^k is selected, where the initial height of v_i is $h_i^0 = l_i = \frac{D_i}{B \cdot \tau}$. Given h_i^{k-1} and the selected set S^k, the value of h_i^k can be calculated by Eq. (25).

Sensor Set Virtualization: Denote by $l_j^{max} = \max\{l_i \mid v_i \in S_j\}$ the maximum value among sensors in S_j. A collection $\mathcal{A}_j = \{A_j^m \mid 1 \leq m \leq l_j^{max}\}$ of virtual sets of S_j is then formed, where each element A_j^m in $\mathcal{A}_j$ contains exactly identical sensors as in S_j and the cardinality of $\mathcal{A}_j$ is l_j^{max}.

Now, each sensor v_i can be regarded as a vertex v_i with the initial height $\frac{D_i}{B \cdot \tau}$, and the union $\cup_{p_j \in \mathcal{P}} \mathcal{A}_j$ can be regarded as the collection of sets in the MCH. Following `Algorithm 2`, within iteration k with $1 \leq k \leq \Gamma$, a set $S_{j^{max}}$ with the maximum value of $\sum_{v_i \in S_{j^{max}} \setminus \mathcal{Y}} min\{h_i^{k-1},\ 1\}$ is selected from

$\cup_{p_j \in \mathcal{P}} \mathcal{A}_j$. Consequently, the identified hovering locations for the UAV are the locations in $\mathcal{P}$ whose virtual set is selected in any iteration, while the hovering duration (in terms of time slots) at each selected location p_j is equal to the number of selected virtual sets of S_j during the Γ iterations. The detailed algorithm for the MOP is given in `Algorithm` 3.

Algorithm 3 Approximation Algorithm for the MOP

Input: A set $\mathcal{V} = \{v_i \mid 1 \leq i \leq N\}$ of sensors; a set $\mathcal{P}$ of potential hovering locations for the UAV; a family $\mathcal{S} = \{S_j \mid p_j \in \mathcal{P}\}$ of data collection sensor sets for the set $\mathcal{P}$ of locations; the maximum number of hovering time slots Γ for the UAV per tour.

Output: $\mathcal{F} = \{(p_j,\ T_j) \mid p_j \in \mathcal{P},\ T_j \geq 1\}$: a set of selected hovering locations for the UAV and the corresponding hovering durations;

1: $\mathcal{F} \leftarrow \emptyset;\ \mathcal{Q} \leftarrow \emptyset$;
2: $\mathcal{T} \leftarrow \{T_j \leftarrow 0 \mid p_j \in \mathcal{P}\}$;
3: **for** each $v_i \in \mathcal{V}$ **do**
4: $\quad l_i \leftarrow \frac{D_i}{B\tau};\ h_i^0 \leftarrow l_i$;
5: **for** each $p_j \in \mathcal{P}$ **do**
6: $\quad l_j^{max} \leftarrow \max_{v_i \in S_j}\{l_i\}$;
7: $\quad$ A collection of virtual sets $\mathcal{A}_j \leftarrow \{A_j^m \mid 1 \leq m \leq l_j^{max}\}$ by duplicating S_j;
8: $\quad \mathcal{Q} \leftarrow \mathcal{Q} \cup \mathcal{A}_j$;
9: **for** $k \leftarrow 1$ to Γ **do**
10: $\quad$ Select a $G_{j^*}^m \in \mathcal{Q}$ with maximum $\sum_{v_i \in G_{j^*}^m} \min\{h_i^{k-1},\ 1\}$;
11: $\quad T_{j^*} \leftarrow T_{j^*} + 1$;
12: $\quad \mathcal{Q} \leftarrow \mathcal{Q} \setminus \{G_{j^*}^m\}$;
13: $\quad$ **for** each $v_i \in \mathcal{V}$ **do**
14: $\quad\quad$ **if** $v_i \in G_{j^*}^m$ **then**
15: $\quad\quad\quad h_i^k \leftarrow \max\{h_i^{k-1} - 1,\ 0\}$;
16: $\quad\quad$ **else**
17: $\quad\quad\quad h_i^k \leftarrow h_i^{k-1}$;
18: **for** each $p_j \in \mathcal{P}$ **do**
19: $\quad$ **if** $T_j \geq 1$ **then**
20: $\quad\quad \mathcal{F} \leftarrow \mathcal{F} \cup \{(p_j,\ T_j)\}$;
21: **return** $\mathcal{F}$.

C. Analysis of the Approximation Ratio

In the following, we analyze the approximation ratios of `Algorithm` 2 and `Algorithm` 3. We use OPT to denote the value of the optimal solution of the MCH. `Algorithm` 2 consists of K iterations, and within each iteration a set with the maximum height decrements is chosen. Denote by p_k and q_k the sum of height decrements at the kth iteration and the total height decrements up to the kth iteration (including the kth iteration), i.e., $q_k = \sum_{m=1}^{k} p_m$. Let g_k be the value difference with OPT after the kth iteration, i.e., $g_k = OPT - q_k$.

Lemma 3:

1) $p_{k+1} \geq \frac{g_k}{K}$, for $k = 0,\ 1,\ \ldots,\ K-1$, where $p_0 = q_0 = 0$, and $g_0 = OPT$.
2) $g_{k+1} \leq (1 - \frac{1}{K})^{k+1} \cdot OPT$, for $k = 0,\ 1,\ \ldots,\ K-1$.

Proof 1) g_k is the value difference from OPT after iteration k with $1 \leq k \leq K$. By the Pigeonhole Principle, one of the K iterations in the optimal solution must be at least $\frac{g_k}{K}$. Since p_{k+1} is the maximum one at time slot $k+1$, we have $p_{k+1} \geq \frac{g_k}{K}$, for $k = 0,\ 1,\ \ldots,\ K-1$.

2) We show this claim by induction. For the base case where $k = 0$, we need to show $g_1 \leq (1 - \frac{1}{K}) \cdot OPT$.

Since $g_k = OPT - q_k$, we have

$$g_1 \leq OPT - q_1 = OPT - p_1 \tag{28}$$
$$\leq OPT - \frac{g_0}{K} \qquad \text{by Lemma 3(1)} \tag{29}$$
$$= OPT - \frac{OPT}{K} = (1 - \frac{1}{K}) \cdot OPT \tag{30}$$

We then show that $g_{k+1} \leq (1 - \frac{1}{K})^{k+1} \cdot OPT$, based on the following inductive hypothesis, that is,

$$g_k \ \leq \ (1 - \frac{1}{K})^k \cdot OPT \tag{31}$$

By induction,

$$g_{k+1} \ = \ g_k - p_{k+1} \ \leq \ g_k - \frac{g_k}{K} \qquad \text{by Lemma 3(1)} \tag{32}$$
$$= \ g_k(1 - \frac{1}{K}) \tag{33}$$
$$\leq \ (1 - \frac{1}{K})^k \cdot OPT \cdot (1 - \frac{1}{K}) \quad \text{by (31)} \tag{34}$$
$$= \ (1 - \frac{1}{K})^{k+1} \cdot OPT \tag{35}$$

□

Theorem 5: The approximation ratio of `Algorithm` 2 for the MOP is $(1 - \frac{1}{e})$.

Proof By Lemma 3, we have shown $g_K \leq (1 - \frac{1}{K})^K \cdot OPT$. Since $(1 - \frac{1}{K})^K \approx \frac{1}{e}$, we have $g_K \leq \frac{OPT}{e}$. Then,

$$q_K = OPT - g_K \ \geq \ OPT - \frac{OPT}{e} \ \geq \ OPT(1 - \frac{1}{e}) \tag{36}$$

where q_K is the profit after the Kth iteration of `Algorithm` 2.

We thus conclude that the approximation ratio of `Algorithm` 2 is $(1 - \frac{1}{e})$. □

Theorem 6: The approximation ratio of `Algorithm` 3 for the MOP is $(1 - \frac{1}{e})$.

Proof Since the sensor height determination and sensor set virtualization never change the volume of data collected at each location in $\mathcal{P}$, the approximation ratio of `Algorithm` 3 is determined by the selection of hovering locations (Step 9 to Step 17 in `Algorithm` 3), which is same as `Algorithm` 2. Therefore, the approximation ratio of `Algorithm` 3 is also $(1 - \frac{1}{e})$ according to Theorem 5. □

VI. Performance Evaluation

In this section, we evaluate the performance of the proposed algorithm by experimental simulations. We also investigate the impact of parameters on the algorithm performance.

A. Experimental Environment Settings

We consider a WSN deployed within $1,000 \times 1,000$ square meters, in which sensors are randomly distributed [7]. The data transmission range and bandwidth of each sensor are set at 150 meters and 1 MB/s [15], respectively. The data volume D_i of each sensor v_i is randomly drawn from $(0,\ 1000]MB$. We employ one UAV for data collection [8], hovering at the altitude 100 meters [3]. The total hovering time of the UAV is set as $1,800$ seconds [13], with the length of each time slot 1 second. Unless otherwise specified, these parameters will be adopted in the default setting. The MOP is a new problem, where existing algorithms in literature are unlikely to be adopted directly due to different data collection models. To evaluate the performance of `Algorithm 1` and `Algorithm 3`, we propose the following benchmark heuristics.

- *Greedy*. It iteratively selects a hovering location p_{max} for the UAV with the maximum volume of collected data, and the UAV hovers at p_{max} until all data from the sensors in S_{max} are collected. This procedure continues until the accumulative hovering duration of the UAV reaches Γ.
- *NSearch*. The UAV firstly hovers at a location p_{max_1} with the maximum volume of collected data, where it collects all data from the sensors in S_{max_1}. It then selects a location p_{max_2} from the neighbors of p_{max_1} (sensors no larger than 225 meters away from location p_{max_1}) where data is also fully collected. The procedure of neighbor selection continues until the UAV runs out of power.
- *UCollect*. The UAV collects data at each hovering location in $\mathcal{P}$ with equal duration, i.e., $\frac{\Gamma}{|\mathcal{P}|}$ number of time slots at each $p_i \in \mathcal{P}$.
- *WCollect*. Denote by $\mathcal{D} = \sum_{p_j \in \mathcal{P}} \sum_{v_i \in S_j} D_i$ the sum of data from all data collection sensor sets (not as same as the total volume of data in the WSN). The hovering duration of the UAV at p_j is decided by the ratio of the volume of data from S_j to $\mathcal{D}$, i.e., $T_j = \Gamma \cdot \frac{\sum_{v_i \in S_j} D_i}{\mathcal{D}}$.

Each value in figures is the mean result by applying each mentioned algorithm to 50 network instances with the same size. The running time of all mentioned experimental simulations is obtained from a desktop with 2.7 GHz Intel Core i5 CPU and 8 GB RAM.

B. Performance Evaluation of Different Algorithms

We first investigate the performance of `Algorithm 1` (denoted by *Alg01*) against heuristics `Greedy`, `NSearch`, `UCollect` and `WCollect` for the MOCP, with 25 randomly distributed potential hovering locations (since the distance between any two locations is required to be strictly larger than $2 \cdot \sqrt{150^2 - 100^2} \approx 225$ meters, the maximum number of potential hovering locations we can generate is around 25). Fig. 5(a) shows that `Alg01` significantly outperforms other heuristics, due to the fact that `Alg01` can always deliver an optimal solution. Fig. 5(b) plots the running time curves of the comparison algorithms.

We then evaluate the performance of `Algorithm 3` (denoted by *Alg03*) against heuristics `Greedy`, `NSearch`, `UCollect` and `WCollect` for the MOP, by varying the number of sensors from 100 to $1,000$, with 100 potential hovering locations. Fig. 6(a) demonstrates that the volume of collected data by all mentioned algorithms is proportional to the network size, due to the fact that with the increase on the number of sensors, more data is generated in the WSN, such that the UAV is able to collect more data at each hovering location. It can also be seen that, the volume of collected data by `Alg03` is approximately 129% of the one by `WCollect`, and 145% of the ones by other heuristics. Fig. 6(b) depicts the time curves of the proposed algorithms.

Note that, `Algorithm 2` just serves as a bridge to solve the MOP. We instead evaluate the performance of `Algorithm 3` directly.

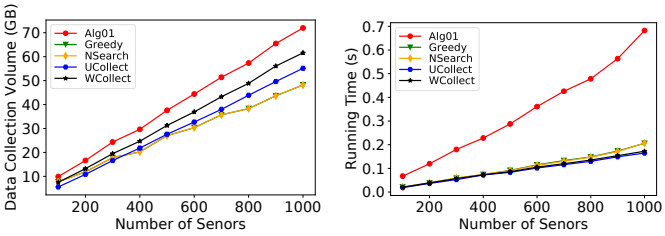

(a) (b)

Fig. 5: Performance of `Alg01`, `Greedy`, `NSearch`, `UCollect` and `WCollect` in WSNs consisting of sensors from 100 to $1,000$.

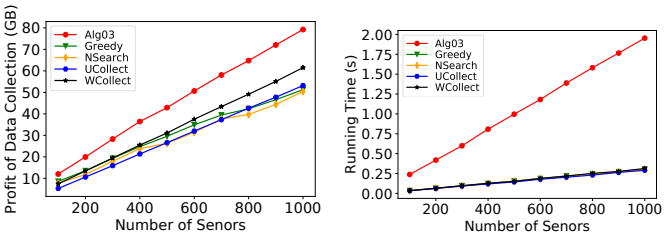

(a) (b)

Fig. 6: Performance of `Alg03`, `Greedy`, `NSearch`, `UCollect` and `WCollect` in WSNs consisting of sensors from 100 to $1,000$.

C. Impact of Parameters on the Performance of Algorithms

The rest is to investigate the impact of the UAV hovering durations and the data transmission range on the performance of the mentioned algorithms, with $1,000$ sensors randomly deployed in the monitoring field.

We first investigate the impact of the UAV hovering duration on the performance of different algorithms, where the number of hovering time slots of the UAV varies from $1,500$ to $2,500$, with length of 1 second. Fig. 7(a) depicts that the volume of collected data delivered by the mentioned algorithms grows rapidly against the hovering time of the UAV, as the UAV is able to collect more data with longer hovering durations. Besides, `Alg03` significantly outperforming others in any cases, where the result of `Alg03` is approximately 123% of

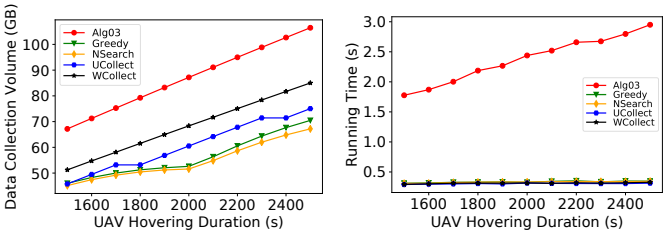

(a) (b)

Fig. 7: Performance of Alg03, Greedy, NSearch, UCollect and WCollect with UAV hovering duration from $1,500$ to $2,500$.

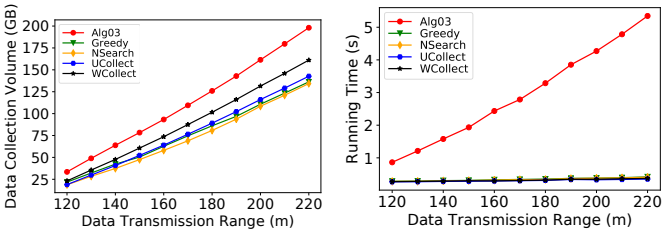

(a) (b)

Fig. 8: Performance of Alg03, Greedy, NSearch, UCollect and WCollect by varying the data transmission range of sensors from 120 meters to 220 meters.

WCollect. From Fig. 7(b), the running time of Alg03 also grows against the number of hovering time slots of the UAV, due to that the number of iterations of Alg03 is determined by the number of UAV hovering time slots.

We then investigate the impact of the data transmission range of sensors on the performance of the mentioned algorithms, by increasing the transmission range from 120 meters to 220 meters (since the transmission range should be larger than the height of the UAV), with $1,000$ sensors randomly deployed in the network. Fig. 8(a) plots that the volume of collected data delivered by different algorithms rises against the data transmission range, due to the fact that the UAV can collect more data with a larger data transmission range of sensors. It also can be seen that the performance gaps between Alg03 and other heuristics become increasingly larger with the growth on the data transmission range. Fig. 8(b) plots the running time curves of the mentioned algorithms. It can be seen from Fig.7 and Fig.8 that the data collection of Alg03 is proportional to the UAV hovering duration and the data transmission range of sensors.

VII. Conclusion

In this paper, we studied data collection in a WSN, using an energy-constrained UAV, where data from multiple sensors can be collected simultaneously by the UAV at any hovering location. We first formulated a novel multi-sensor data collection optimization problem and showed that the problem is NP-hard. We then devised an efficient approximation algorithm with a constant approximation ratio for it. We finally evaluated the proposed algorithm through experimental simulations. Simulation results demonstrate that the proposed algorithm is promising, and outperforms other heuristics significantly.

Acknowledgements

It is acknowledged that the work by Mengyu Chen, Weifa Liang and Yuchen Li was supported by the Australian Research Council Discovery Project No. DP200101985.

References

[1] H. Binol, E. Bulut, K. Akkaya, and I. Guvenc. Time optimal multi-uavpath planning for gathering its data from roadside units. *Proc of 88th Vehicular Technology Conference* (VTC-Fall), IEEE, pp. 1–5, 2018.

[2] M. B. Ghorbel, D. Rodriguez-Duarte, H. Ghazzai, M. J. Hossain, and H. Menouar. Energy efficient data collection for wireless sensors using drones. *Proc of 87th VTC Spring*, pp. 1–5, IEEE, 2018.

[3] J. Gong, T. Chang, C. Shen and X. Chen. Flight time minimization of UAV for data collection over wireless sensor networks. *Journal on Selected Areas in Communications*, vol. 36, no. 9, pp. 1942–1954, 2018.

[4] J. Guo, T. Wang, Y. He, M. Jin, C. Jiang and Y. Liu. TwinLeak: RFID-based liquid leakage detection in industrial environments. *Proc. of INFOCOM'19*, pp. 883–891, IEEE, 2019.

[5] P. Kodeswaran, R. Kokku, M. Mallick and S. Sen. Demultiplexing activities of daily living in IoT enabled smarthomes. *Proc. 35th INFOCOM'16*, pp. 1-9, IEEE, 2016.

[6] M. Li and H.-J. Lin. Design and implementation of smart home control systems based on wireless sensor networks and power line communications. *IEEE Transactions on Industrial Electronics*, vol. 62, no. 7, pp.4430 – 4442, 2015.

[7] Y. Li, W. Liang, W. Xu, and X. Jia. Data collection of IoT devices using an energy-constrained UAV. To appear in *Proc. 34th IPDPS'20*, IEEE, 2020.

[8] Y. Liang, W. Xu, W. Liang, J. Peng, X. Jia, Y. Zhou, and L. Duan. Nonredundant information collection in rescue applications via an energy-constrained uav. *IEEE Internet of Things Journal*, vol. 6, no. 2, pp. 2945–2958, 2018.

[9] C. Lin, C. Guo, H. Dai, L. Wang and G. Wu. Near optimal charging scheduling for 3-D wireless rechargeable sensor networks with energy constraints. *Proc. 39th ICDCS'19*, pp. 624–633, IEEE, 2019.

[10] C. Luo, X. Feng, J. Chen, J. Li, W. Xu, W. Li, L. Zhang, Z. Tari and A. Y. Zomaya. Brush like a dentist: accurate monitoring of toothbrushing via wrist-worn gesture sensing. *Proc of INFOCOM'19*, pp. 1234–1242, IEEE, 2019.

[11] M. Mozaffari, W. Saad, M. Bennis, and M. Debbah. Mobile internet of things: Can uavs provide an energy-efficient mobile architecture? *Proc of GLOBECOM'16*, pp. 1–6, IEEE, 2016.

[12] M. Mozaffari, W. Saad, M. Bennis, Y.-H. Nam, and M. Debbah. A tutorial on uavs for wireless networks: Applications, challenges, and open problems. *IEEE Communications Surveys & Tutorials*, 2019.

[13] Phantom 4 specification. (2017) [Online]. Available: https://www.dji.com/au/phantom-4-adv/info.

[14] M. Samir, S. Sharafeddine, C. Assi, T. Nguyen, and A. Ghrayeb. Uav trajectory planning for data collection from time-constrained iot devices. *IEEE Transactions on Wireless Communications*, vol.19, no.1, pp. 34–46, 2020.

[15] J. Theunissen, H. Xu, R. Y. Zhong and X. Xu. Smart AGV system for manufacturing shopfloor in the Context of Industry 4.0. *25th Proc of M2VIP'18,* pp. 1-6, 2018.

[16] V. Di Valerio, F. Lo Presti, C. Petrioli, L. Picari, D. Spaccini and S. Basagni. CARMA: Channel-aware reinforcement learning-based multi-path adaptive routing for underwater wireless sensor networks. *IEEE Journal on Selected Areas in Communications*, vol. 37, no. 11, pp. 2634–2647, 2019.

[17] C. Zhan, Y. Zeng, and R. Zhang. Energy-efficient data collection in uav enabled wireless sensor network. *IEEE Wireless Communications Letters*, vol. 7, no. 3, pp. 328–331, 2017.